






Review

Technological Aspects and Performance of High Entropy Alloys with Potential Application in Dental Restorations and Reducing Implant Failure

Ioana Demetrescu ^{1,2}, Radu Nartita ¹, Mihai Andrei ³, Andreea Cristiana Didilescu ^{3,*}, Anisoara Cimpean ⁴ and Daniela Ionita ¹

¹ Department of General Chemistry, Bucharest National Polytechnic University of Science and Technology, 313 Splaiul Independentei, 060042 Bucharest, Romania; ioana.demetrescu@upb.ro (I.D.); nartita.radu@gmail.com (R.N.); daniela.ionita@upb.ro (D.I.)

² Academy of Romanian Scientists, 3 Ilfov, 050044 Bucharest, Romania

³ Division of Embryology, Faculty of Dental Medicine, Carol Davila University of Medicine and Pharmacy, 050474 Bucharest, Romania; mihai.andrei@umfcd.ro

⁴ Department of Biochemistry and Molecular Biology, University of Bucharest, 91–95 Splaiul Independentei, District 5, 050095 Bucharest, Romania; anisoara.campean@gmail.com

* Correspondence: andreea.didilescu@umfcd.ro

Abstract: Amidst the prevalence of aggressive bacterial infections that can impact both oral and systemic health following various dental and implant procedures, the search for alternative, high-performing and biocompatible materials has become a challenging pursuit. The need for such investigations is increasing owing to the fact that toxicological risks of cobalt–chromium (CoCr) alloys used in dentistry have become a part of the EU’s new Medical Devices Regulations establishing that cobalt metal has been classified as carcinogenic, genotoxic and detrimental to reproduction. Within this context, this review proposes high entropy alloys (HEA) as potential alternatives and presents their characteristics and in vitro biological performance when used as a substrate or coating. Anatomical details of the oral cavity in relationship with prosthodontics and implant dentistry support the paper’s motivation and presentation. The review highlights the innovative manufacturing procedures, microstructure and properties of both the bulk and coatings of BioHEA. It evaluates the performance of BioHEAs based on their complete characterization and assesses their suitability for novel applications in dentistry, serving as the primary objective of this manuscript.

Keywords: dental HEAs; dental restorations; implant failure



Citation: Demetrescu, I.; Nartita, R.; Andrei, M.; Didilescu, A.C.; Cimpean, A.; Ionita, D. Technological Aspects and Performance of High Entropy Alloys with Potential Application in Dental Restorations and Reducing Implant Failure. *Appl. Sci.* **2023**, *13*, 12000. <https://doi.org/10.3390/app132112000>

Academic Editors: Eriberto A. Bressan, Luca Sbricoli and Riccardo Guazzo

Received: 19 September 2023

Revised: 22 October 2023

Accepted: 1 November 2023

Published: 3 November 2023



Copyright: © 2023 by the authors. Licensee MDPI, Basel, Switzerland. This article is an open access article distributed under the terms and conditions of the Creative Commons Attribution (CC BY) license (<https://creativecommons.org/licenses/by/4.0/>).

1. Introduction

Over time, metallic alloys have been increasingly used in restorative works and implants to address anatomical degradation and dental health issues [1]. In dentistry, they are most commonly used in prosthodontics as fixed restorations and removable partial dentures. Prosthetic restorations perform the function of replacing teeth by restoring their morphology following tooth loss due to various pathological processes. Dental alloys are used for fixed prosthetic manufacturing as complete cast, metal–ceramic (porcelain fused to metal) crowns or bridges (Figure 1a), for overdentures, telescopic crowns (Figure 1b,d) and removable partial denture metal frameworks (Figure 1c) [2].

Dental alloys can be classified as gold-based, palladium-based, silver-based, nickel-based, titanium-based, cobalt-based or iron-based alloys [3]. Low price; good corrosion resistance due to electro-chemical stability; and desirable mechanical traits, including considerable strength, a high modulus of elasticity and low flexibility, have made non-precious nickel–chromium and cobalt–chromium alloys widely used for dental metal frameworks [4,5]. A distinguished category of dental alloys is titanium-based alloys used for manufacturing dental implants. Dental implants are biomedical devices, most commonly

obtained industrially, that act as a substitute for the natural tooth root; they are placed in the maxilla or mandible bones, where they undergo osseointegration. Unlike dental implants, fixed prosthetic restorations and removable partial dentures metal frameworks are obtained in the dental laboratory by various technological processes, from traditional casting to modern technologies; for example, subtractive techniques such as CAD/CAM (computer-aided design and computer-aided manufacturing) or additive manufacturing such as 3D metal printing (selective laser melting (SLM), direct metal laser sintering (DMLS)) [6–8]. All metal frameworks in Figure 1 are DMLS 3D printed.

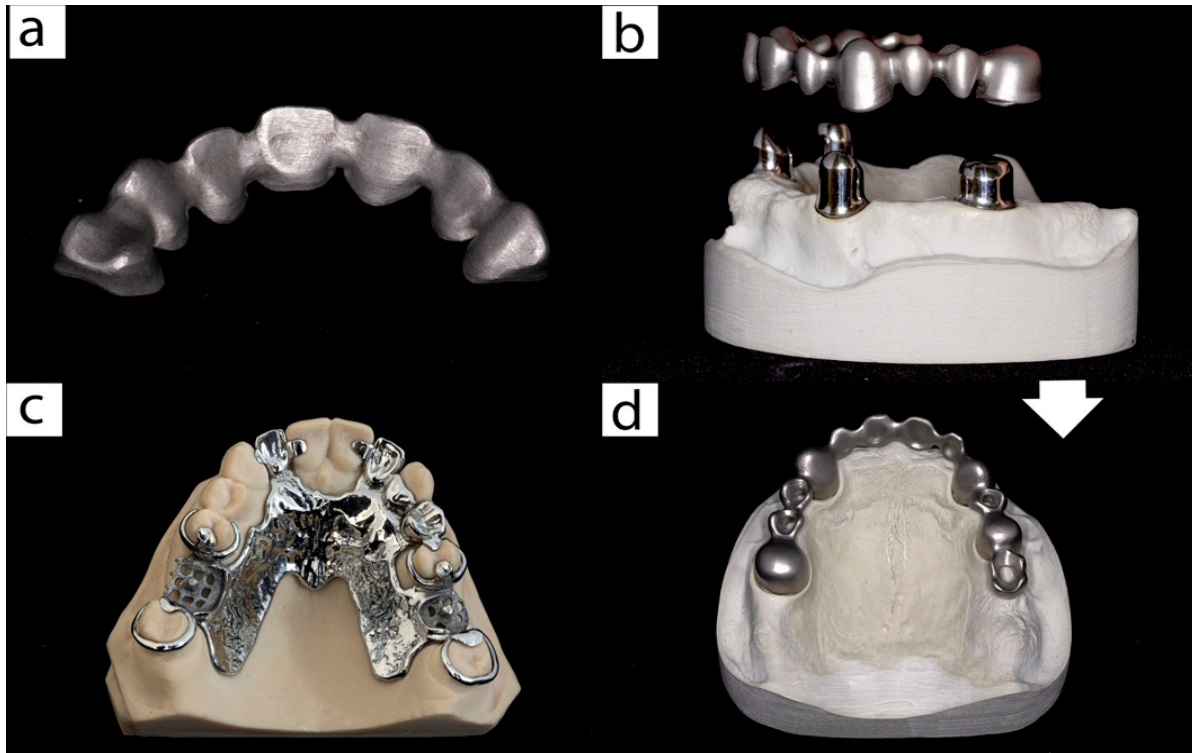


Figure 1. Three-dimensional printing technology of CoCr metal frameworks for fixed and removable restorations: (a) a metal framework for a metal–ceramic fixed partial denture; (b,d) a metal overdenture framework with telescopic crowns; (c) a metal framework for an upper removable partial denture.

While significant progress has been made in researching metallic materials, from stainless steel to titanium, zirconium [9] and noble alloys [1,10,11], a material that can be used with no associated risk or need for revision after several years has yet to be discovered. Conventional implants face two problems: biocompatibility degradation due to ion release, which can be caused by chemical corrosion or wear, and a mismatch of mechanical properties, which can cause stress shielding [12]. The bone structure, which is formed by cortical dental plates, has cortical porosity with regional differences and a complex network of intracortical canals. This structure is inversely proportional with regard to mechanical characteristics like bone strength and stiffness [13]. Despite the good properties of the metallic biomaterials used in restorative works and implants, both coated and uncoated [14–16], it is still challenging to find suitable materials that present no risk of implant failure [17].

One promising alloy that could be used in dental arch wires due to its shape memory properties, superelasticity and elastic modulus close to that of the bone is the NiTi alloy. However, the potential release of Ni ions and their associated allergic and carcinogenic effects are concerning [18,19]. Similar concerns are associated with the CoCrMo medium entropy alloy, which has a good combination of mechanical properties and resistance to

corrosion, making it a good candidate as dental implant material. Cr ions cause several problems if they reach the bloodstream, such as DNA lesions, causing an increased cancer risk. However, it was observed that Cr oxides formed naturally on the surface of this alloy prevent the release of Cr ions upon corrosion and that Co and Mo ions are more easily released [15].

Considering the harmful effects of cobalt and the allergic reactions that ensue from nickel [20], which can lead to health risks owing to the release of toxic ions, restrictions have been placed on their use in dentistry. This has led to investigations into finding alternative materials and the need to eliminate CoCr and nickel–chromium (NiCr) alloys from dentistry [21]. Research has estimated that nickel allergy affects more than 28.5% of the general population, which is considered a high potential risk for health [22,23]. As a result, the toxicological risks of cobalt–chromium alloys in dentistry have become a part of the EU Medical Devices Regulation (MDR) (2017/745), which was scheduled to be fully implemented in May 2021 [24]. According to this EU regulation, cobalt metal has been associated with carcinogenic properties, mutagenic effects and reproductive toxicity [25]. The EU MDR regulation entered into application on 26 May 2021. However, due to global events such as the pandemic, the full implementation of medical device regulation (MDR) has been delayed until December 2022. The new regulation has introduced changes such as the reclassification of existing products and requirements for more clinical trials.

In the quest for the perfect equilibrium between biocompatibility, strength, resistance to corrosion and wear, much of the latest research is focused on high entropy alloys (HEAs) [26–32]. Due to the sensitive nature of the European regulatory changes surrounding the use of CoCr dental alloys [25], the strategy to reduce their toxicological risk has become a challenge for BioHEA investigations. The BioHEAs studied are mainly composed of elements that are common in biocompatible binary and ternary alloys, such as Ti, Zr, Ta, Nb and Mo, which are known for their high cytocompatibility, good strength and increased corrosion resistance [17]. Particularly, the Ti-Zr-based BioHEAs possess high strength and good wear resistance, making them suitable to be used as screws due to their resistance to deformation and fracture [33].

Dental alloy restorations are designed to last for years in the patient’s oral cavity, an environment that often contributes to the slow or accelerated degradation of these metal biomaterials. However, it must be taken into account that such biomedical devices must be safe in use so that, in the long term, they do not initiate and/or maintain biocompatibility issues [34]. Most of the time, problems occur as a result of corrosion that leads to metal ions release, which can migrate locally or systemically in the body, leading to undesirable adverse effects [35]. An important factor in achieving long-term clinical success is the nature of the alloy from which the restoration is manufactured. Regarding dental implants, integration problems occur at the interfaces with soft and hard tissues in the form of mucositis (an inflammatory process of the soft tissue surrounding the implant) [36] and peri-implantitis (an inflammatory process of the implant’s surrounding connective tissue followed by osseous support loss) [37], which may require complex and costly re-interventions such as tissue regeneration [38], and in severe cases, implant rejection may occur.

In the case of HEA implant materials, there are not only obvious drawbacks related to the costs of such materials but also technical, such as poor castability [26] and elemental segregation [39]. Several strategies are being researched and evaluated to address these issues, such as HEA coatings on cheaper substrates and different fabrication methods with highly controlled parameters [40–44].

Elements such as Ag and Cu can also be used when designing HEA for antimicrobial properties. However, the antimicrobial mechanism, in this case, is based mainly on the ion release, which may affect the mechanical properties and resistance to corrosion in addition to other possible negative effects on cells and living tissue [45,46]. The present manuscript presents the manufacturing procedures, microstructure and properties of the bulk BioHEAs

and BioHEA coatings used in dental applications. Its main objective is to support the scientific motivation and oral health highlighted in the paper.

2. Data Sources and Search Strategy

For this review, we considered only review and original articles written in English that were related to the use of high entropy alloys as biomaterials, especially dental alloys. Several searches were conducted in databases such as PubMed, Scopus and MDPI using the keywords: “BioHEA”, “high entropy alloy implant”, “dental high entropy alloys”, etc. After conducting the initial search, we identified a total of 89 articles based on their titles and abstracts. Of these, 31 were excluded after full reading due to either their lack of relevance or insufficient data provided.

The aim was to summarize the most promising high entropy alloys that have been studied while taking into consideration all the relevant aspects for assessing their use as dental implants, such as mechanical properties, corrosion resistance and cell behavior. Moreover, we also addressed the drawbacks and highlighted possible mitigating strategies.

3. The Oral Cavity Relationship with Prosthodontics and Implant Dentistry

In terms of the relationship with the oral tissues, metal-based frameworks create interfaces with the oral tissues. Fixed restorations are long-term attached to the teeth with a specific dental luting cement that cannot be self-removed by the patient. Fixed prostheses come in contact with the prepared teeth abutments (especially dentin) and, respectively, their surrounding gingiva (marginal periodontium) [47]. In the case of removable partial dentures, the metal-based structure (dental base) comes into contact with the denture-supporting tissues such as the edentulous alveolar ridge and its covering masticatory mucosa and with anatomical elements such as the hard palate and its covering mucosa (the major connector of the partial removable denture) [48]. Retentive elements of the framework (direct or indirect retainers, rests) may establish contact with the abutment teeth in order to obtain a well-fitting denture with high stability and retention to resist displacement [49].

Knowledge of the oral cavity’s anatomical structures, muscle insertions, aspects of innervation, vascularization and related anatomical structures are necessary to avoid risks and complications following endosseous implant placement [50]. Dental materials are subject to general requirements similar to other biomaterials. Biocompatibility, mechanical properties and corrosion resistance are essential considerations, and their quantitative values depend on the manufacturing process and reprocessing needs [51].

4. BioHEAs

4.1. Bulk

The class of high entropy alloys was introduced based on the idea that when the entropic contribution surpasses the enthalpic value, the formation of intermetallic phases is suppressed, leading to system stabilization. Incorporating less common elements with unique properties in a small amount, typically less than 5%, generates a state of local disorder that contributes to exceptional properties such as enhanced resistance to corrosion, oxidation and abrasion [52,53]. These alloys, composed of multiple elements, exhibit special mechanical and thermal properties, including high strength, hardness, toughness and ultra-high fracture toughness [42]. The well-selected combination of elements in specific ratios leads to properties such as unique corrosion resistance in bioliquids and superior biocompatibility [54]. The most used manufacturing techniques are presented in Figure 2, along with some key characteristics and BioHEAs that have been prepared using them.

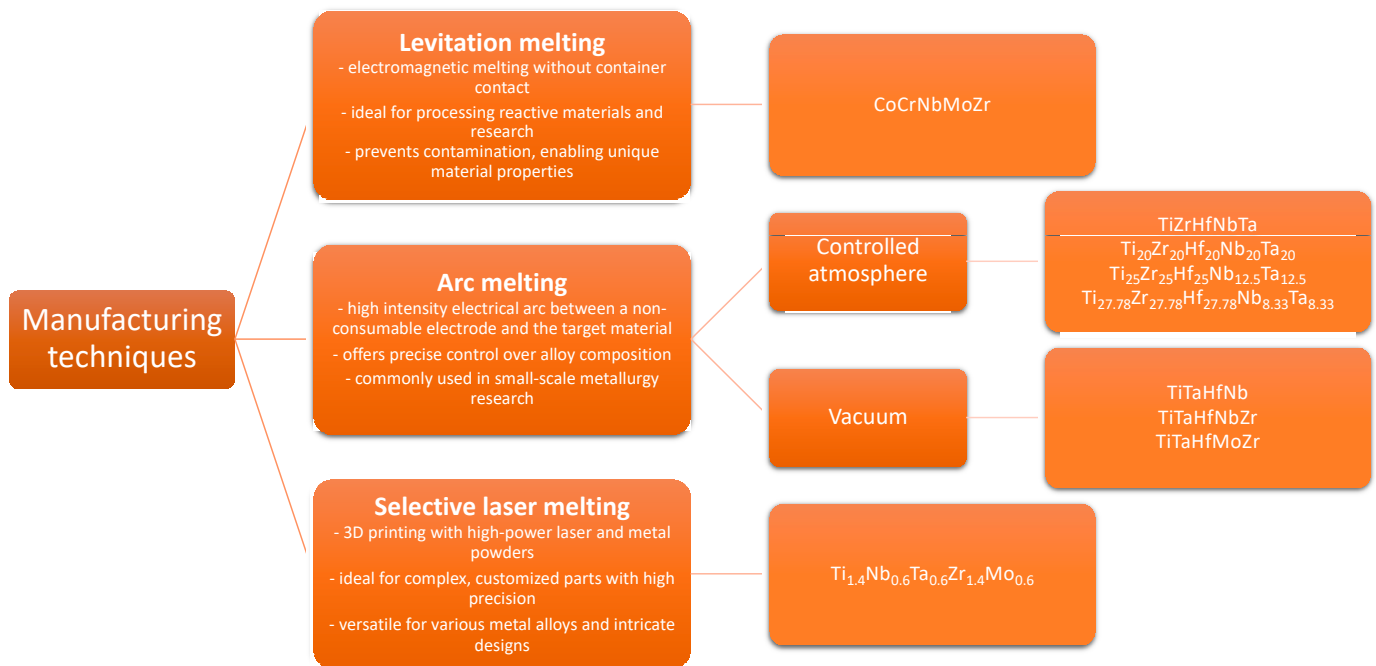


Figure 2. Manufacturing technologies used to fabricate bulk BioHEAs.

Although the number of research on BioHEAs, particularly on BioHEAs used in dentistry, has gained momentum in recent years [55–59], the researchers began to involve more elements in traditional alloys even earlier. Drob et al. enriched the commercial CoCrMo alloy with 6% Nb and 0.8% Zr, thus lowering Young’s modulus from 228 GPa to 108 GPa, which is very close to that of the maxilla bone, while also measuring an improved resistance to corrosion [60].

More recently, the TiZrHfNbTa alloy was prepared by Yang et al. through arc-melting of the pure metals. The authors have studied the bio-corrosion in Hank’s solution and evaluated the biocompatibility using MC3T3-E1 pre-osteoblasts in parallel with the Ti6Al4V. The results indicate that the HEA alloy tested presents both good corrosion resistance and biocompatibility, similar to that of Ti6Al4V. Additionally, it does not pose a risk associated with Al and V ions release and has a lower elastic modulus of approx. 80 GPa compared to 110 GPa [61].

The same alloy was also recently prepared by Zhang et al., who studied the effect of plasma electrolytic oxidation as a surface treatment at different voltages. It was observed that the alloy performance can be improved in terms of wear and corrosion resistance without hindering cell adhesion and proliferation [62]. Another popular surface treatment [63–65], investigated on this alloy by Berger et al., is the development of self-arranged oxide nanotubes through anodization in an electrolyte solution containing F^- ions, showing good mechanical, corrosion resistance and bioactivity [66].

Other non-equiatomic HEAs were also developed, including $Ti_{25}Zr_{25}Hf_{25}Nb_{12.5}Ta_{12.5}$ and $Ti_{27.78}Zr_{27.78}Hf_{27.78}Nb_{8.33}Ta_{8.33}$ with an even lower Young’s modulus of 68 GPa and 56 GPa, respectively. The alloys have also displayed good corrosion resistance and biocompatibility, favoring the adhesion and proliferation of MC3T3-E1 cells [67].

The biocompatibility of TiZrHf and $Ti_{40}Zr_{20}Hf_{10}Nb_{20}Ta_{10}$ was also studied by investigating their behavior in 3.5% NaCl and studying the attachment, proliferation and genetic expression of human gingival fibroblasts (HGFs). While the TiZrHf was shown to be susceptible to pitting corrosion, the corrosion resistance of the quinary alloy was superior compared to both TiZrHf and CP-Ti. Moreover, both alloys were proven to be superior in terms of biocompatibility, showing no cytotoxicity, with the quinary alloy being the most effective in inducing the proliferation of HGFs and improving the gene expression of adhesion factors compared with CP-Ti [68].

Following thermodynamic calculations, Iijima et al. predicted that introducing Mo in a smaller amount would still lead to solid solution formation and have thus developed a nonequiatomic HEA, $\text{Ti}_{28.33}\text{Zr}_{28.33}\text{Hf}_{28.33}\text{Nb}_{6.74}\text{Ta}_{6.74}\text{Mo}_{1.55}$. The biocompatibility of this HEA assessed in osteoblast culture proved to be higher than in the case of Co-Cr-Mo and slightly superior to that of CP-Ti, which is frequently utilized for orthopedic and dental implants [69].

Other BioHEAs for which the biocompatibility was proven to be comparable to that of CP-Ti were developed using a treelike diagram starting from TiZrHf and the commercially available CoCrMo, obtaining $\text{TiZrHfCr}_{0.2}\text{Mo}$ and $\text{TiZrHfCo}_{0.07}\text{Cr}_{0.07}\text{Mo}$ [70].

Besides the arc melting preparation method, which appears to be the common choice for BioHEAs, SLM was also proposed and used to fabricate $\text{Ti}_{1.4}\text{Nb}_{0.6}\text{Ta}_{0.6}\text{Zr}_{1.4}\text{Mo}_{0.6}$. The authors postulated that by significantly increasing the cooling rate to 10^5 – 10^7 K/s, the probability of elemental segregation will be lowered. Moreover, the material's biocompatibility was evaluated by using primary osteoblasts and compared to the same alloy prepared through arc melting, observing that the uniform distribution in the SLM alloy led to an increased cell density [39].

Hashimoto et al. prepared and analyzed several BioHEAs, looking for Ni-free shape memory alloys and identifying the most promising candidate among those studied, the $(\text{TiZrHf})_{82}\text{Nb}_5\text{Ta}_5\text{Al}_8$ alloy. The alloy was found to be superelastic, with low magnetic susceptibility, good biocompatibility and corrosion resistance [71].

Iron, which is inexpensive, may also be added to improve the resistance to wear and corrosion, as shown by Wang et al. in the case of the developed TiZrHfNbFe alloy. Despite the fact that the microhardness increases with the Fe content, as well as the resistance to wear, they observed that the smallest amount tested of Fe (0.5 molar ratio) provided the best corrosion resistance in PBS, without traces of pitting corrosion [72].

Several BioHEAs studied as bulk are presented in Table 1, along with their microstructure and properties.

Table 1. Microstructure and properties of the bulk BioHEAs.

Alloy Studied	Microstructure	Mechanical Properties	Resistance to Corrosion	Reference
TiZrHfNbTa	BCC structure	n/a	Corrosion rate— 5.6×10^{-4} mm/year (Hank's solution) Ion concentration after 28 days of immersion in Hank's solution: Ti—19.8 ppb Zr—1.4 ppb Hf—0.76 ppb Nb—8.4 ppb Ta—9.8 ppb	[61]
$\text{Ti}_{28.33}\text{Zr}_{28.33}\text{Hf}_{28.33}\text{Nb}_{6.74}\text{Ta}_{6.74}\text{Mo}_{1.55}$	BCC structure	Higher mechanical strength than CP-Ti observed through the stress–strain curve	n/a	[69]
$\text{TiZrHfCr}_{0.2}\text{Mo}$	BCC dendritic structure with minor interdendritic phases	HV—531		[70]
$\text{TiZrHfCo}_{0.07}\text{Cr}_{0.07}\text{Mo}$		HV—532		
$\text{Ti}_{40}\text{Zr}_{20}\text{Hf}_{10}\text{Nb}_{20}\text{Ta}_{10}$	BCC structure	HV—294 E—86.4 GPa	The polarization behavior in 3.5% NaCl indicates significantly higher corrosion resistance compared with CP-Ti	[68]

Table 1. Cont.

Alloy Studied	Microstructure	Mechanical Properties	Resistance to Corrosion	Reference
Ti ₂₀ Zr ₂₀ Hf ₂₀ Nb ₂₀ Ta ₂₀	Single BCC solid solution	HV—320 E—79 GPa	Corrosion rate— 5.5×10^{-4} mm/year (Hank's solution)	
Ti ₂₅ Zr ₂₅ Hf ₂₅ Nb _{12.5} Ta _{12.5}		HV—293 E—68 GPa	Corrosion rate— 8.8×10^{-4} mm/year (Hank's solution)	[67]
Ti _{27.78} Zr _{27.78} Hf _{27.78} Nb _{8.33} Ta _{8.33}		HV—287 E—56 GPa	Corrosion rate— 9.3×10^{-4} mm/year (Hank's solution)	
CoCrNbMoZr	bi-phase of two hexagonally Co-based phases	E—107.88 GPa	R _p —251.9 kΩcm ² (saliva pH = 3.83) R _p —751.4 kΩcm ² (saliva pH = 7.84) R _p —163.3 kΩcm ² (saliva pH = 9.11) R _p —206.5 kΩcm ² (saliva + 0.05 M NaF pH = 8.21)	[60]
TiTaHfNb		n/a	Ion concentration after 28 days immersion in fetal bovine serum (FBS): Ti—309.32 ppb Ta—1.14 ppb Nb—0.87 ppb Total ion concentration after 28 days of immersion in: —artificial saliva (AS): approx. 70 ppb —in simulated body fluid (SBF): approx. 20 ppb	
TiTaHfNbZr	BCC structure		Ion concentration after 28 days of immersion in FBS: Ti—347.24 ppb Ta—9.34 ppb Nb—29.86 ppb Zr—10.76 ppb Total ion concentration after 28 days of immersion in: —AS: approx. 70 ppb —SBF: approx. 15 ppb	[12,73]
TiTaHfMoZr			Ion concentration after 28 days of immersion in FBS: Ti—309.32 ppb Ta—9.45 ppb Mo—162.49 ppb Zr—4.39 ppb Total ion concentration after 28 days of immersion in: —AS: approx. 200 ppb —SBF: approx. 70 ppb	
Ti _{1.4} Nb _{0.6} Ta _{0.6} Zr _{1.4} Mo _{0.6}	BCC solid solution	E—140 GPa	n/a	[39]

4.2. Coatings

Coated biomaterials, utilized extensively in various medical applications, should ideally exhibit a combination of specific properties to ensure their effectiveness and biocompatibility. Firstly, these coatings must possess superior biocompatibility to prevent adverse reactions when in contact with living tissues or bodily fluids. Moreover, they should encourage cellular adhesion and growth, facilitating tissue integration and regeneration. Additionally, the coatings must exhibit suitable mechanical properties, providing the necessary strength and flexibility to withstand physiological forces without compromising the structural integrity of the biomaterial. They should also be resistant to degradation, ensuring prolonged functionality within the body. Finally, the surface of the coated biomaterial should ideally be designed to minimize bacterial adhesion and biofilm formation, thereby reducing the risk of infections and promoting long-term implant success. These properties are depicted in Figure 3.

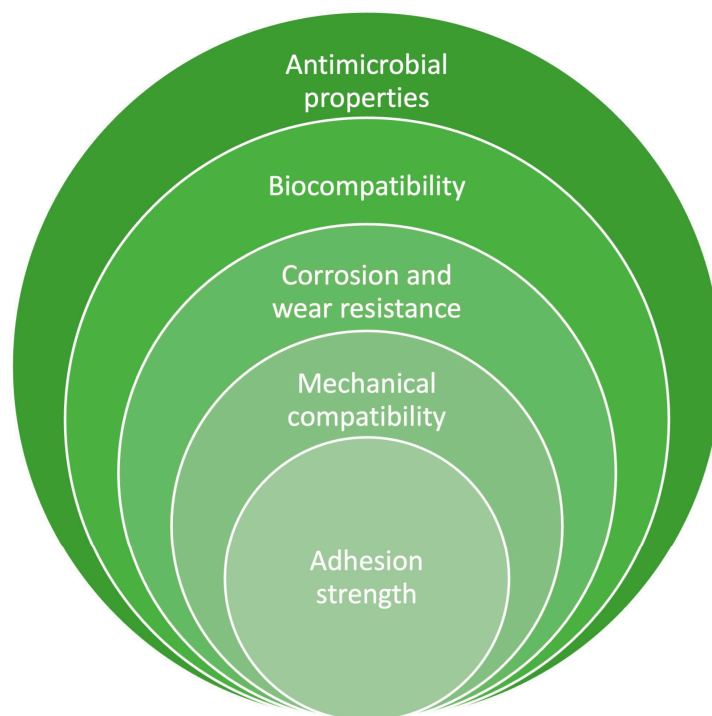


Figure 3. Desired properties of alloys coated with BioHEAs.

The passive oxide film formed naturally on some alloys helps to increase the resistance to corrosion and acts as a barrier for the release of cytotoxic metal ions. However, due to wear, local areas may appear where the substrate is exposed. The galvanic coupling then formed between the passivated and depassivated zone causes the acceleration of corrosion. This may also happen between a coating and the substrate; therefore, it is highly important to develop coatings with superior adhesion [26].

Research on corrosion is thus conducted using complex environments that would mimic those found in the human body. One such study conducted on TiTaHfNb, TiTaHfNbZr and TiTaHfMoZr HEAs in fetal bovine serum (FBS) showed hydroxyapatite formation on their surface, especially on the TiTaHfNb alloy. This alloy also presents the lowest elastic modulus of the three, 112.2 GPa [12]. The same alloys were also tested in simulated body fluid (SBF) and artificial saliva (AS), observing that the addition of Zr and Nb increased the resistance to corrosion while the addition of Mo increased the ion release in both media upon immersion [73].

One approach proposed by Aksoy et al. to reduce the Ni ions released from the NiTi alloy is by coating it with the TiTaHfNbZr alloy. They studied the corrosion of this coated alloy in two very acid media, artificial saliva (pH = 2.3) and gastric fluid (pH = 2), through immersion over a period of 28 days, showing a significant reduction in Ni concentration in both fluids, but an increasing trend was still observed [19]. Motallebzadeh also measured the release of Ni ions over a period of 28 days, but in SBF, and noted a significantly lower concentration from 265.6 ppb in the case of the uncoated alloy to 1.9 ppb in the case of the coated alloy, with a coating thickness of 750 nm [18].

The HEA composed of $Ti_{1.5}ZrTa_{0.5}Nb_{0.5}Hf_{0.5}$ was evaluated as coating after being deposited on different substrates, such as 316 L, CoCrMo and Ti6Al4V by RF magnetron sputtering. Although the hardness was significantly increased in all three cases, both 316L and CoCrMo presented fairly poor adhesion, and delamination was observed at approximately 200 mN and 290 mN, respectively. Additionally, both coated alloys showed pitting behavior in the PBS solution. However, the coated Ti6Al4V presented superior adhesion, without delamination and increased passivation, without pitting traces [26]. The same coating, but with equimolar composition, was also studied on Ti6Al4V, observing that the coated specimen had increased resistance to wear and cracking [74].

Several BioHEAs studied as coatings are presented in Table 2, along with their preparation method, substrate used, microstructure and properties.

Table 2. Microstructure and properties of the BioHEAs coatings.

Coating Studied	Substrate Used	Microstructure	Mechanical Properties	Resistance to Corrosion	Reference
Ti _{1.5} ZrTa _{0.5} Nb _{0.5} Hf _{0.5}	316L	Amorphous structure Roughness—2.05 nm	H—11.43 GPa E—180 GPa Critical load—190 mN	Rp (Tafel)— $78.2 \times 10^4 \Omega\text{cm}^2$ (PBS) Rfilm (EIS)— $5.10 \times 10^4 \Omega\text{cm}^2$ (PBS) Rct (EIS)— $4.25 \times 10^6 \Omega\text{cm}^2$ (PBS)	[26]
	CoCrMo	Amorphous structure Roughness—2.11 nm	H—11.49 GPa E—185 GPa Critical load—280 mN	Rp (Tafel)— $81.8 \times 10^4 \Omega\text{cm}^2$ (PBS) Rfilm (EIS)— $6.10 \times 10^4 \Omega\text{cm}^2$ (PBS) Rct (EIS)— $6.95 \times 10^6 \Omega\text{cm}^2$ (PBS)	
	Ti6Al4V	Amorphous structure Roughness—2.27 nm	H—11.49 GPa E—183 GPa Critical load—>400 mN	Rp (Tafel)— $83.0 \times 10^4 \Omega\text{cm}^2$ (PBS) Rfilm (EIS)— $8.43 \times 10^4 \Omega\text{cm}^2$ (PBS) Rct (EIS)— $1.54 \times 10^7 \Omega\text{cm}^2$ (PBS)	
TiTaHfNbZr	Ti6Al4V	Amorphous structure Roughness—2.78 nm	H—12.51 GPa E—181.3 GPa	n/a	[74]
TiTaHfNbZr	NiTi	Amorphous structure	HV—1285 E—183.2 GPa	Lower Ni ion concentration after 28 days of immersion both in artificial saliva (pH = 2.3) and gastric fluid (pH = 2) for the coated samples	[19]
TiTaHfNbZr	NiTi	750 nm coating thickness Roughness—4.35 nm	H—12.44 GPa E—182.8 GPa Critical load—158 mN	1.88 ppb Ni after 28 days immersion in SBF compared to 265.55 ppb Ni for uncoated alloy	[18]
		1500 nm coating thickness Roughness—4.35 nm	H—11.82 GPa E—175.1 GPa Critical load—204 mN	n/a	

5. In Vitro Biological Performance of HEA

Thus far, most of the tests to evaluate the biological performance of HEAs rely on cell culture experiments by direct cell contact methods, as it is further described. However, although the majority of these tests envisaged the demonstration of the HEA suitability for orthopedic implants, these studies can be expanded to applying these alloys for dental implants since in vitro responses of bone-derived cells have been mainly investigated (Table 3).

Table 3. In vitro biological performance of the designed BioHEAs.

BioHEA Studied	Investigated Cell Type	In Vitro Biological Performance	Quantitative Assessments	Reference
Non-equiatomic BioHEAs (Ti _{1.4} Zr _{1.4} Nb _{0.6} Ta _{0.6} Mo _{0.6})	Human osteoblasts	Cell morphology and density are similar to CP-Ti and equiatomic TiNbTaZrMo but higher than on SUS-316L surface. More mature focal adhesions than on SUS-316L.	Size regulation of fibrillar adhesions: 810/mm ²	[75]
As-cast and SLM-built Ti _{1.4} Nb _{0.6} Ta _{0.6} Zr _{1.4} Mo _{0.6} BioHEAs	Mouse primary neonatal calvarial osteoblasts	Comparable biological performance to CP-Ti but superior to SS316L in terms of cell density, morphology and spreading as well as osteogenic differentiation. The SLM process showed the most promising potential.	Cell density: >8000 cells/cm ²	[39]
Ti _{28.33} Zr _{28.33} Hf _{28.33} Nb _{6.74} Ta _{6.74} Mo _{1.55} (at.%) (TZHNTM-3)	Mouse primary neonatal calvarial osteoblasts	Similar biological performance to CP-Ti but superior to SUS316L and Co-Cr-Mo in terms of osteoblast cytomorphology, adhesion and spreading, as well as cytoskeleton organization	Cell density: ~8000 cells/cm ²	[69]
TiZrHfCr _{0.2} Mo TiZrHfCo _{0.07} Cr _{0.07} Mo	Mouse primary neonatal calvarial osteoblasts	Superior in vitro biocompatibility (enhanced cell adhesion, widespread morphology, mature focal adhesions) comparable to that of CP-Ti and higher than that exhibited by SUS316 and Co-Cr-Mo commercial alloys.	Cell density: ~9000 cells/cm ²	[70]
Ti ₂₀ Zr ₂₀ Hf ₂₀ Nb ₂₀ Ta ₂₀	MC3T3-E1 mouse pre-osteoblast cell line	In vitro cellular response comparable to Ti6Al4V alloy (morphology characteristic to healthy cells, enhanced pre-osteoblast adhesion, high levels of cell viability and proliferation)	Cell viability after 7 days incubation: ~100%	[61]
Ti ₂₀ Zr ₂₀ Hf ₂₀ Nb ₂₀ Ta ₂₀ Ti ₂₅ Zr ₂₅ Hf ₂₅ Nb _{12.5} Ta _{12.5} (Alloy-II) Ti _{27.78} Zr _{27.78} Hf _{27.78} Nb _{8.33} Ta _{8.33} (Alloy-III)	MC3T3-E1 mouse pre-osteoblast cell line	Good cell adhesion, high cell viability and proliferation, which were equivalent to those exhibited by the Ti6Al4V alloy	Cell numbers attached: 95–105% *	[67]
MoNbTaTiZr	HW-MSCs; MC3T3-E1 pre-osteoblast cell line	Improved in vitro biocompatibility in terms of cell adhesion and survival rate, migratory potential and osteogenic commitment when compared to SS304 alloy	Cell viability: 89.31%	[76]
Dual-phase MoNbTaTiZr (HEA); HEA-FSP, HEA-SFP	HW-MSCs	Conditioned media collected by incubation of the processed samples showed better cell viability and proliferation than that exhibited by the extraction media of SS316L and Ti6Al4V materials. HEA-SFP displayed the highest biological performance	Cell viability: 90–95%	[54]
Ti ₄₀ Zr ₂₀ Hf ₁₀ Nb ₂₀ Ta ₁₀	Human primary gingival fibroblasts (HGF)	Greater biological performance in terms of HGF adhesion (cell attachment, spreading and gene expression of some cell adhesion factors), viability and proliferation than TiZrHf and, especially, CP-Ti	Quantitative real-time PCR assay: enhanced expression of VEGFA, COL1a, COL5a, FN1 and MMP9	[68]
Ti ₅₀ Zr ₂₅ Nb ₂₀ Cu _{2.5} Ag _{2.5} HEA	MC3T3-E1 pre-osteoblast cell line	Higher capacity to induce the osteogenic differentiation of MC3T3-E1 pre-osteoblasts than Ti4Al6V by increasing the expression of osteogenesis-related genes and alkaline phosphatase activity	Antibacterial rate: 99%	[77]

* expressed as percentage of cells attached to Ti6Al4V.

The cell behavior was investigated especially at the early stages of cell-surface interactions like cell attachment and spreading as well as cell proliferation (Figure 4, created with BioRender.com (accessed on 22 April 2023) as indicators of the materials' biological performance. For instance, Todai et al. developed a novel equiatomic TiNbTaZrMo HEA and investigated its cytocompatibility with human osteoblasts in terms of cellular morphology, spreading and density in comparison to 316 L stainless steel (SUS-316L) and CP-Ti as reference biomaterials [78].

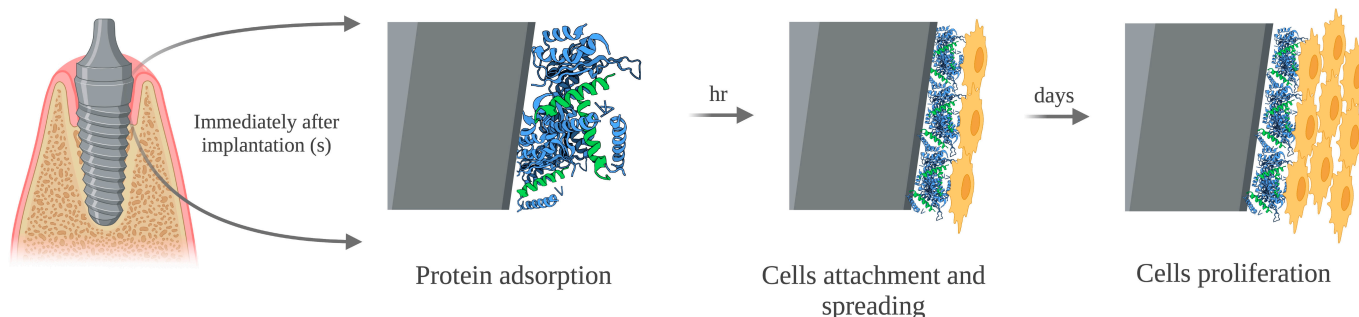


Figure 4. Stages of the cell-material surface interactions investigated during the process of evaluation of HEA in vitro biological performance.

It was found that the osteoblasts on the surfaces of this BioHEA, both under as-cast and annealed forms, exhibit an extensive morphology akin to the cellular morphology on CP-Ti as well as a significantly higher number of cells than SUS-316 L, showing promising potential as a new class of metallic bioalloys. On the other hand, Hori et al. developed four compositions of non-equiatomic Ti-Nb-Ta-Zr-Mo BioHEA and showed that the osteoblasts in contact with $\text{Ti}_{1.4}\text{Zr}_{1.4}\text{Nb}_{0.6}\text{Ta}_{0.6}\text{Mo}_{0.6}$ exhibited a widespread morphology and a cell density that was resembling that of the cells observed on CP-Ti and equiatomic TiNbTaZrMo but higher than on SUS-316L surface [75]. Moreover, on this BioHEA surface, more mature focal adhesions could be noticed as compared to osteoblasts in contact with the SUS-316L sample. Also, the focal adhesions were significantly longer than in the cells on $\text{Ti}_{0.6}\text{Zr}_{0.6}\text{Nb}_{1.4}\text{Ta}_{1.4}\text{Mo}_{1.4}$, suggesting that $\text{Ti}_{1.4}\text{Zr}_{1.4}\text{Nb}_{0.6}\text{Ta}_{0.6}\text{Mo}_{0.6}$ was the most potent in stimulating the focal adhesions maturation in the osteoblast cells.

It is well known that the maturation of focal adhesions is closely associated with tissue integration of the implanted biomaterials [79], and this finding proves that the non-equiatomic $\text{Ti}_{1.4}\text{Zr}_{1.4}\text{Nb}_{0.6}\text{Ta}_{0.6}\text{Mo}_{0.6}$ BioHEA possessed a superior in vitro biological performance when compared to that of SUS-316L alloy. This study brings to attention that by manipulating the alloy compositions in the Ti-Nb-Ta-Zr-Mo bioHEAs, implant biocompatibility can be optimized. This study has also demonstrated that the features of the oxide layer from the interface between cells and the metallic substrate play an important role in influencing cell behavior. Thus, as evinced by the XPS analysis, the oxide layer on the SFP specimen is rich in ZrO_2 , which is known to be highly biocompatible and supports cell viability and multiplication.

The same research group investigated pre-alloyed $\text{Ti}_{1.4}\text{Nb}_{0.6}\text{Ta}_{0.6}\text{Zr}_{1.4}\text{Mo}_{0.6}$ BioHEA powders and SLM-built parts with low porosity and demonstrated that the cell density on the SLM-built sample was similar to that on the conventional CP-Ti biomaterial and the cast counterpart but significantly higher when compared to that on SS316L [39]. Likewise, the fluorescent images of the actin cytoskeleton and focal adhesions exhibited by the osteoblasts adhered to the SLM-processed HEA samples revealed a widespread morphology with a dense actin filament network similar to those on CP-Ti. Therefore, the uniform compositional distribution of the SLM-built samples endows them with advantages for cell spreading, which was demonstrated to be a biophysical cue playing a critical role in the osteogenic commitment and differentiation of stem cells [80]. On the contrary, due to elemental segregation in cast counterpart, the distribution of filopodia in osteoblasts was restricted by gripping the adhesion spots in Ti- and Zr-enriched inter-dendrite regions, leading to reduced cell spreading. Overall, both as-cast and $\text{Ti}_{1.4}\text{Nb}_{0.6}\text{Ta}_{0.6}\text{Zr}_{1.4}\text{Mo}_{0.6}$ proved to show more promising potential for biomedical applications than SS316L. Moreover, based on the above results showing the suitability of the $\text{Ti}_{1.4}\text{Nb}_{0.6}\text{Ta}_{0.6}\text{Zr}_{1.4}\text{Mo}_{0.6}$ for bone implants, Nagase et al. developed novel TiZrHfCr_{0.2}Mo and TiZrHfCo_{0.07}Cr_{0.07}Mo HEAs by a combination of Ti-Nb-Ta-Zr-Mo alloy system and Co-Cr-Mo alloy system as accepted biomaterial for surgical implants and dental alloys [70]. The in vitro cytocompatibility of these BioHEAs with mouse primary osteoblasts isolated from neonatal calvariae (cell

density, cytomorphological features, actin cytoskeleton organization and focal adhesions maturation) was equivalent to CP-Ti and superior to SUS-316 and Co-Cr-Mo commercial alloys, demonstrating their application as bone implants with multiple functions.

As already presented, Iijima et al. developed a $\text{Ti}_{28.33}\text{Zr}_{28.33}\text{Hf}_{28.33}\text{Nb}_{6.74}\text{Ta}_{6.74}\text{Mo}_{1.55}$ BioHEA and studied its behavior in vitro in comparison to CP-Ti, SUS316L stainless steel and Co-Cr-Mo as reference metallic biomaterials [69]. Cell adhesion and densities of the primary osteoblasts isolated from neonatal mouse calvarial bone and incubated for 24 h in contact with the analyzed samples were significantly lower on SUS316L and Co-Cr-Mo substrates than on CP-Ti and TZHNTM-3 surfaces, as assessed by Giemsa staining. Furthermore, microscopic images acquired after fluorescent labeling of actin cytoskeleton and vinculin (protein enriched in focal adhesions) evinced that the osteoblasts in contact with the surfaces of SUS316L and Co-Cr-Mo alloys exhibit reduced spreading and altered cytoskeletal organization. On the contrary, the cells that adhered to the TZHNTM-3 surface exhibited a widespread morphology and densely packed actin filaments quite similar to the osteoblasts grown on CP-Ti substrate. Altogether, these results demonstrated that the developed BioHEA is significantly more suitable than SUS-316 L and the Co-Cr-Mo alloy for bone tissue regeneration and possesses similar cytocompatibility to CP-Ti. This finding is also supported by its low cytotoxicity derived from high corrosion resistance and the formation of a protective and bioactive oxide layer.

In another study performed on MC3T3-E1 mouse pre-osteoblasts seeded on the surface of the equimolar $\text{Ti}_{20}\text{Zr}_{20}\text{Hf}_{20}\text{Nb}_{20}\text{Ta}_{20}$ HEA, Yang et al. investigated the substrate cellular colonization by using MTT assay and expressing the percentage of cell viability relative to negative control over a culture period of 7 days [61]. In addition, the number of attached cells was semiquantitatively evaluated by their staining with live/dead kit. For comparative purposes, the cellular response to the conventional Ti6Al4V alloy was assessed. It was found that on both alloys, the cells expressed high and similar cell viability levels and proliferation rates. Moreover, SEM images indicated that these alloys support the good adhesion and the healthy state of MC3T3-E1 pre-osteoblasts, suggesting the similar biosafety of the TiZrHfNbTa HEA and the Ti6Al4V alloy. In a more recent paper, Yang et al. comparatively evaluated in vitro pre-osteoblast response to this HEA bioalloy (Alloy-I), $\text{Ti}_{25}\text{Zr}_{25}\text{Hf}_{25}\text{Nb}_{12.5}\text{Ta}_{12.5}$ (Alloy-II) and $\text{Ti}_{27.78}\text{Zr}_{27.78}\text{Hf}_{27.78}\text{Nb}_{8.33}\text{Ta}_{8.33}$ (Alloy-III) [67]. These HEAs exhibited an increased number of adhered MC3T3-E1 cells and high cellular viability and proliferation, which were comparable to those displayed by the conventional Ti6Al4V alloy, demonstrating their great potential for biomedical applications.

Shittu et al. investigated the in vitro behavior of human Wharton's jelly-derived mesenchymal stem cells (HW-MSCs) and MC3T3-E1 pre-osteoblasts (ATCC CRL-2593) grown in contact with the equiatomic MoNbTaTiZr HEA [76]. Thus, on this surface, HW-MSCs exhibited a high cell viability percentage (89%) and a larger cellular body when compared to the control surface (tissue culture polystyrene (TCPS)), suggesting its high potential to support cell adhesion and growth. To investigate the compatibility of this HEA with pre-osteoblast cells, a parallel study was carried out on the SS304 stainless steel. The cellular morphological examination by SEM and fluorescence microscopy revealed smaller cells on this surface with elongated shapes and relatively fewer filopodia extensions when compared to MC3T3-E1 cells in contact with MoNbTaTiZr HEA. On this last material, a cellular monolayer represented by elongated and spindle-shaped pre-osteoblasts was evinced, exhibiting a migratory phenotype with leading and trailing edges and several filopodial extensions as well as actin filament bundles that are crucial for the cell adhesion and proper functioning of cells.

Altogether, these in vitro results confirmed the highly biocompatible nature of the MoNbTaTiZr bioHEA. It is worth noting that several members of the same research team previously reported on the behavior of HW-MSCs cultured in the conditioned media from dual-phase HEA comprising the same elements (MoNbTaTiZr) in comparison to conditioned media derived from conventional metallic biomaterials, namely, SS316L and Ti6Al4V [54]. This alloy underwent extensive surface deformation using stationary friction

processing (SFP) and friction stir processing (FSP) to homogenize its microstructure. MTT assay performed on cells cultured in the conditioned media from HEA, HEA-FSP, and HEA-SFP revealed that higher cell viability was induced by the processed HEAs when compared to its as-cast counterpart, SS316L and Ti6Al4V conventional materials. It was found that all alloys are biocompatible with a cell viability of 85% and over; e.g., the HEA-SFP sample exhibited better cell viability (95%), comparable to that of the cells grown in complete media (control cells). Furthermore, fluorescence microscopy images revealed the exclusive presence of live cells. Thus, it was concluded that the HEA, HEA-FSP and HEA-SFP do not exhibit acute toxicity, all of these samples demonstrating good biocompatibility as implant biomaterials.

These results are not surprising since they are in accordance with previous data reported by Hori et al. and Todai et al. regarding the MoNbTaTiZr bioHEA's in vitro biocompatibility following elemental homogenization through 168 h furnace annealing [75,78]. The superior biological performance of the SFP sample was ascribed to the characteristics of the oxide layer at cell–metallic substrate interface. Specifically, the oxide layer for this specimen was enriched in ZrO₂ and was already presented to promote cell viability and proliferation as well as more homogeneous and stable. This last study was based on indirect contact cell-based tests.

The only available study on the in vitro behavior of human gingival fibroblasts (HGFs) on HEAs was reported by Wang et al. [68]. They comparatively investigated the biocompatibility of the single-phase body-centered cubic (BCC) structured Ti₄₀Zr₂₀Hf₁₀Nb₂₀Ta₁₀ BioHEA and single-phase hexagonal close-packed (HCP) equiatomic TiZrHf and CP-Ti conventional reference biomaterial. The fibroblasts in contact with the HEA alloy exhibited enhanced adhesion when compared to TiZrHf and, especially, CP-Ti surfaces, as shown by the increased number of the attached cells, cytoplasmic and filopodial extensions, and more rapid and wider cellular spreading and the genetic expression levels of multiple cell adhesion factors like vascular endothelial growth factor A (VEGFa), matrix metalloproteinase-9 (MMP-9), collagen type 1a (COL1a), collagen type 5a (COL5a) and fibronectin 1 (FN1) indicating the reduction in wound healing times. CCK-8 assay showed the presence of a higher number of metabolically active viable cells in contact with the Ti₄₀Zr₂₀Hf₁₀Nb₂₀Ta₁₀ than on the TiZrHf and CP-Ti surfaces, suggesting the enhanced capacity of the analyzed BioHEA to sustain increased viability and proliferation of the HGFs. This finding was also supported by the results of the CCK-8 assay performed on the leaching solutions of these biomaterials, indicating that the newly designed BioHEA is more compatible with HGF cells than TiZrHf and especially CP-Ti, holding great potential for dental applications.

The above in vitro studies have not yet approached the expression of cell-type specific markers, but the HEA's capacity to support cell differentiation was predicted by assessing the changes induced in cells' sizes and shapes following direct contact with the materials' surfaces. However, a recent paper by Yu et al. reports on the potential of the Ti₅₀Zr₂₅Nb₂₀Cu_{2.5}Ag_{2.5} HEA to induce osteogenic differentiation of MC3T3-E1 pre-osteoblasts grown in contact with its surface by studying the gene expression and activity of alkaline phosphatase (ALP) known as an early marker of osteoblast differentiation, as well as mRNA levels of bone morphogenetic protein (BMP)-2 as an osteoinductive factor. This study was comparatively performed on the Ti6Al4V alloy, and the results obtained revealed lower intracellular ALP activity and mRNA expression levels of ALP and BMP-2 than those exhibited by Ti₅₀Zr₂₅Nb₂₀Cu_{2.5}Ag_{2.5} on the 7th day of culture, suggesting its superior bioactivity [77].

In summary, despite the recent progress in designing new metallic materials with promising potential in the biomedical field, like HEAs, there is still room for improvement in the assessment of their biological performance since mainly cell culture-based studies have been developed so far. To the best of our knowledge, Akmal et al. investigated the in vivo biocompatibility of HEAs from the Mo–Ta–Nb–Ti–Zr system, specifically the (MoTa)_{0.2}NbTiZr that was implanted in the thigh muscles of ten-week-old male C57BL/6 mice in the shape of cylindrical rods. The histological evaluation of the respective

muscle at four weeks indicated that the implant did not induce any toxicity or muscle damage, suggesting the biosafety of this HEA [81]. Likewise, Yu et al.'s model showed very recently that $\text{Ti}_{50}\text{Zr}_{25}\text{Nb}_{20}\text{Cu}_{2.5}\text{Ag}_{2.5}$ HEA exhibits enhanced biocompatibility and higher antibacterial properties than the conventional Ti6Al4V alloy, indicating its suitability for the peri-implant tissue regeneration [77].

6. Conclusions

While significant strides have been achieved in the exploration of various metallic materials in the medical field, the search for an ideal biomaterial continues. Challenges such as biocompatibility degradation due to ion release and the mismatch of mechanical properties persist in conventional implants. Moreover, regulatory restrictions on the use of certain alloys, such as cobalt–chromium and nickel–chromium, have necessitated the exploration of alternative materials.

The emergence of BioHEAs has shown promise, particularly in addressing the limitations associated with traditional alloys, offering improved corrosion resistance, biocompatibility and mechanical strength. Notwithstanding the progress made, there remains a need for comprehensive in vivo studies to further evaluate the biological performance and long-term efficacy of these alloys in diverse biomedical applications. It is imperative to continue exploring novel fabrication techniques and surface treatments to enhance the properties and mitigate the limitations of these biomaterials for sustained biocompatibility and improved clinical outcomes.

Author Contributions: Conceptualization, R.N., M.A., A.C.D., A.C., D.I. and I.D.; methodology A.C.D., A.C., D.I. and I.D.; software, R.N. and M.A.; formal analysis, M.A.; investigation, R.N. and M.A.; resources, D.I.; data curation, A.C.; writing—original draft preparation, R.N., M.A. and A.C.; writing—review and editing, A.C.D., A.C., D.I. and I.D.; visualization, R.N.; supervision, A.C.D. and I.D.; funding acquisition, D.I. and I.D. All authors have read and agreed to the published version of the manuscript.

Funding: This research was funded by the Executive Agency for Higher Education, Research, Development and Innovation Funding, grant number PN-III-P2-2.1-PED-2021-2884 (605PED/2022).

Acknowledgments: We would like to thank Dental Depot for providing the metal framework restorations presented in Figure 1.

Conflicts of Interest: The authors declare no conflict of interest.

References

1. Tharani Kumar, S.; Prasanna Devi, S.; Krithika, C.; Raghavan, R. Review of metallic biomaterials in dental applications. *J. Pharm. Bioallied Sci.* **2020**, *12*, 14. [[CrossRef](#)] [[PubMed](#)]
2. Han, X.; Sawada, T.; Schille, C.; Schweizer, E.; Scheideler, L.; Geis-Gerstorfer, J.; Rupp, F.; Spintzyk, S. Comparative Analysis of Mechanical Properties and Metal-Ceramic Bond Strength of Co-Cr Dental Alloy Fabricated by Different Manufacturing Processes. *Materials* **2018**, *11*, 1801. [[CrossRef](#)] [[PubMed](#)]
3. Messer, R.; Wataha, J. Dental Materials: Biocompatibility. In *Encyclopedia of Materials: Science and Technology*; Elsevier: Amsterdam, The Netherlands, 2002; pp. 1–10.
4. de Matos, J.D.M.; Dos-Santos, A.C.M.; Nakano, L.J.N.; De-Vasconcelos, J.E.L.; Andrade, V.C.; Nishioka, R.S.; Bottino, M.A.; da Rocha Scalzer Lopes, G. Metal Alloys in Dentistry: An Outdated Material or Required for Oral Rehabilitation? *Int. J. Odontostomatol.* **2021**, *15*, 702–711. [[CrossRef](#)]
5. Reclaru, L.; Lüthy, H.; Eschler, P.-Y.; Blatter, A.; Susz, C. Corrosion behaviour of cobalt–chromium dental alloys doped with precious metals. *Biomaterials* **2005**, *26*, 4358–4365. [[CrossRef](#)] [[PubMed](#)]
6. Kim, H.; Jang, S.H.; Kim, Y.; Son, J.; Min, B.; Kim, K.H.; Kwon, T.Y. Microstructures and Mechanical Properties of Co-Cr Dental Alloys Fabricated by Three CAD/CAM-Based Processing Techniques. *Materials* **2016**, *9*, 596. [[CrossRef](#)]
7. Cabrita, J.; Mendes, T.; Martins, J.; Lopes, L. Removable partial denture metal framework manufactured by selective laser melting technology—A clinical report. *Rev. Port. Estomatol. Med. Dentária Cir. Maxilofac.* **2021**, *62*, 109–113. [[CrossRef](#)]
8. Venkatesh, K.V.; Nandini, V.V. Direct Metal Laser Sintering: A Digitised Metal Casting Technology. *J. Indian Prosthodont. Soc.* **2013**, *13*, 389–392. [[CrossRef](#)]
9. Romonti, D.E.; Gomez Sanchez, A.V.; Milošev, I.; Demetrescu, I.; Ceré, S. Effect of anodization on the surface characteristics and electrochemical behaviour of zirconium in artificial saliva. *Mater. Sci. Eng. C* **2016**, *62*, 458–466. [[CrossRef](#)]

10. Davis, R.; Singh, A.; Jackson, M.J.; Coelho, R.T.; Prakash, D.; Charalambous, C.P.; Ahmed, W.; da Silva, L.R.R.; Lawrence, A.A. A comprehensive review on metallic implant biomaterials and their subtractive manufacturing. *Int. J. Adv. Manuf. Technol.* **2022**, *120*, 1473–1530. [CrossRef]
11. Gueye, M.; Ammar-Merah, S.; Nowak, S.; Decorse, P.; Chevillot-Biraud, A.; Perrière, L.; Couzinie, J.P.; Guillot, I.; Dirras, G. Study of the stability under in vitro physiological conditions of surface silanized equimolar HfNbTaTiZr high-entropy alloy: A first step toward bio-implant applications. *Surf. Coat. Technol.* **2020**, *385*, 125374. [CrossRef]
12. Gurel, S.; Nazarahari, A.; Canadinc, D.; Cabuk, H.; Bal, B. Assessment of biocompatibility of novel TiTaHf-based high entropy alloys for utility in orthopedic implants. *Mater. Chem. Phys.* **2021**, *266*, 124573. [CrossRef]
13. Giesen, E.B.W.; Van Eijden, T.M.G.J. The Three-dimensional Cancellous Bone Architecture of the Human Mandibular Condyle. *J. Dent. Res.* **2000**, *79*, 957–963. [CrossRef] [PubMed]
14. Liu, R.; Li, X.; Hu, X.; Dong, H. Surface modification of a medical grade Co-Cr-Mo alloy by low-temperature plasma surface alloying with nitrogen and carbon. *Surf. Coat. Technol.* **2013**, *232*, 906–911. [CrossRef]
15. Gurel, S.; Nazarahari, A.; Canadinc, D.; Gerstein, G.; Maier, H.J.; Cabuk, H.; Bukulmez, T.; Cananoglu, M.; Yagci, M.B.; Toker, S.M.; et al. From corrosion behavior to radiation response: A comprehensive biocompatibility assessment of a CoCrMo medium entropy alloy for utility in orthopedic and dental implants. *Intermetallics* **2022**, *149*, 107680. [CrossRef]
16. Ionita, D.; Man, I.; Demetrescu, I. The Behaviour of Electrochemical Deposition of Phosphate Coating on CoCr Bio Alloys. *Key Eng. Mater.* **2007**, *330–332*, 545–548. [CrossRef]
17. Feng, J.; Tang, Y.; Liu, J.; Zhang, P.; Liu, C.; Wang, L. Bio-high entropy alloys: Progress, challenges, and opportunities. *Front. Bioeng. Biotechnol.* **2022**, *10*, 977282. [CrossRef]
18. Motallebzadeh, A. Evaluation of mechanical properties and in vitro biocompatibility of TiZrTaNbHf refractory high-entropy alloy film as an alternative coating for TiO₂ layer on NiTi alloy. *Surf. Coat. Technol.* **2022**, *448*, 128918. [CrossRef]
19. Aksoy, C.B.; Canadinc, D.; Yagci, M.B. Assessment of Ni ion release from TiTaHfNbZr high entropy alloy coated NiTi shape memory substrates in artificial saliva and gastric fluid. *Mater. Chem. Phys.* **2019**, *236*, 121802. [CrossRef]
20. Olms, C.; Yahiaoui-Doktor, M.; Remmerbach, T.W. Contact allergies to dental materials. *Swiss Dent. J.* **2019**, *129*, 571–579.
21. Al-Imam, H.; Benetti, A.R.; Özhayat, E.B.; Pedersen, A.M.L.; Johansen, J.D.; Thyssen, J.P.; Jellesen, M.S.; Gotfredsen, K. Cobalt release and complications resulting from the use of dental prostheses. *Contact Dermat.* **2016**, *75*, 377–383. [CrossRef]
22. Zigante, M.; Rincic Mlinaric, M.; Kastelan, M.; Perkovic, V.; Trinajstic Zrinski, M.; Spalj, S. Symptoms of titanium and nickel allergic sensitization in orthodontic treatment. *Prog. Orthod.* **2020**, *21*, 17. [CrossRef] [PubMed]
23. Hostýnek, J.J.; Reagan, K.E.; Maibach, H.I. Nickel Allergic Hypersensitivity: Prevalence and Incidence by Country, Gender, Age, and Occupation. In *Nickel and the Skin*; CRC Press: Boca Raton, FL, USA, 2002; pp. 39–82.
24. Regulation (EU) 2017/745 of the European Parliament and of the Council of 5 April 2017 on Medical Devices. Available online: <https://eur-lex.europa.eu/legal-content/EN/TXT/?uri=CELEX%3A32017R0745> (accessed on 14 April 2023).
25. Grosogeat, B.; Vaicelyte, A.; Gauthier, R.; Janssen, C.; Le Borgne, M. Toxicological Risks of the Cobalt–Chromium Alloys in Dentistry: A Systematic Review. *Materials* **2022**, *15*, 5801. [CrossRef]
26. Peighambardoust, N.S.; Alamdari, A.A.; Unal, U.; Motallebzadeh, A. In vitro biocompatibility evaluation of Ti_{1.5}ZrTa_{0.5}Nb_{0.5}Hf_{0.5} refractory high-entropy alloy film for orthopedic implants: Microstructural, mechanical properties and corrosion behavior. *J. Alloys Compd.* **2021**, *883*, 160786. [CrossRef]
27. Wang, H.; Liu, P.; Chen, X.; Lu, Q.; Zhou, H. Mechanical properties and corrosion resistance characterization of a novel Co36Fe36Cr18Ni10 high-entropy alloy for bioimplants compared to 316L alloy. *J. Alloys Compd.* **2022**, *906*, 163947. [CrossRef]
28. George, E.P.; Raabe, D.; Ritchie, R.O. High-entropy alloys. *Nat. Rev. Mater.* **2019**, *4*, 515–534. [CrossRef]
29. Miracle, D.B.; Senkov, O.N. A critical review of high entropy alloys and related concepts. *Acta Mater.* **2017**, *122*, 448–511. [CrossRef]
30. Miracle, D.B. High entropy alloys as a bold step forward in alloy development. *Nat. Commun.* **2019**, *10*, 1805. [CrossRef]
31. Normand, J.; Moriche, R.; García-Garrido, C.; Sepúlveda Ferrer, R.E.; Chicardi, E. Development of a TiNbTaMoZr-Based High Entropy Alloy with Low Young's Modulus by Mechanical Alloying Route. *Metals* **2020**, *10*, 1463. [CrossRef]
32. Nguyen, V.T.; Qian, M.; Shi, Z.; Tran, X.Q.; Fabijanic, D.M.; Joseph, J.; Qu, D.D.; Matsumura, S.; Zhang, C.; Zhang, F.; et al. Cuboid-like nanostructure strengthened equiatomic Ti–Zr–Nb–Ta medium entropy alloy. *Mater. Sci. Eng. A* **2020**, *798*, 140169. [CrossRef]
33. Hua, N.; Wang, W.; Wang, Q.; Ye, Y.; Lin, S.; Zhang, L.; Guo, Q.; Brechtel, J.; Liaw, P.K. Mechanical, corrosion, and wear properties of biomedical Ti–Zr–Nb–Ta–Mo high entropy alloys. *J. Alloys Compd.* **2021**, *861*, 157997. [CrossRef]
34. Elshahawy, W.; Watanabe, I. Biocompatibility of dental alloys used in dental fixed prosthodontics. *Tanta Dent. J.* **2014**, *11*, 150–159. [CrossRef]
35. Haugli, K.H.; Syverud, M.; Samuelsen, J.T. Ion release from three different dental alloys—Effect of dynamic loading and toxicity of released elements. *Biomater. Investig. Dent.* **2020**, *7*, 71–79. [CrossRef] [PubMed]
36. Heitz-Mayfield, L.J.A.; Salvi, G.E. Peri-implant mucositis. *J. Clin. Periodontol.* **2018**, *45*, S237–S245. [CrossRef] [PubMed]
37. Schwarz, F.; Derks, J.; Monje, A.; Wang, H.-L. Peri-implantitis. *J. Clin. Periodontol.* **2018**, *45*, S246–S266. [CrossRef] [PubMed]
38. Andrei, M.; Dinischiotu, A.; Didilescu, A.C.; Ionita, D.; Demetrescu, I. Periodontal materials and cell biology for guided tissue and bone regeneration. *Ann. Anat. Anat. Anz.* **2018**, *216*, 164–169. [CrossRef]

39. Ishimoto, T.; Ozasa, R.; Nakano, K.; Weinmann, M.; Schnitter, C.; Stenzel, M.; Matsugaki, A.; Nagase, T.; Matsuzaka, T.; Todai, M.; et al. Development of TiNbTaZrMo bio-high entropy alloy (BioHEA) super-solid solution by selective laser melting, and its improved mechanical property and biocompatibility. *Scr. Mater.* **2021**, *194*, 113658. [[CrossRef](#)]
40. Rashidy Ahmady, A.; Ekhlasi, A.; Nouri, A.; Haghbin Nazarpak, M.; Gong, P.; Solouk, A. High entropy alloy coatings for biomedical applications: A review. *Smart Mater. Manuf.* **2023**, *1*, 100009. [[CrossRef](#)]
41. Ozerov, M.; Sokolovsky, V.; Nadezhdin, S.; Zubareva, E.; Zhrebtsova, N.; Stepanov, N.; Huang, L.; Zhrebtsov, S. Microstructure and mechanical properties of medium-entropy TiNbZr alloy-based composites, reinforced with boride particles. *J. Alloys Compd.* **2023**, *938*, 168512. [[CrossRef](#)]
42. Nartita, R.; Ionita, D.; Demetrescu, I.; Enachescu, M. A fresh perspective on medium entropy alloys applications as coating and coating substrate. *Ann. Acad. Rom. Sci. Ser. Phys. Chem.* **2022**, *7*, 34–46. [[CrossRef](#)]
43. Sharma, A. High Entropy Alloy Coatings and Technology. *Coatings* **2021**, *11*, 372. [[CrossRef](#)]
44. Dobbstein, H.; Gurevich, E.L.; George, E.P.; Ostendorf, A.; Laplanche, G. Laser metal deposition of compositionally graded TiZrNbTa refractory high-entropy alloys using elemental powder blends. *Addit. Manuf.* **2019**, *25*, 252–262. [[CrossRef](#)]
45. Zhou, E.; Qiao, D.; Yang, Y.; Xu, D.; Lu, Y.; Wang, J.; Smith, J.A.; Li, H.; Zhao, H.; Liaw, P.K.; et al. A novel Cu-bearing high-entropy alloy with significant antibacterial behavior against corrosive marine biofilms. *J. Mater. Sci. Technol.* **2020**, *46*, 201–210. [[CrossRef](#)]
46. Prodana, M.; Ionita, D.; Stoian, A.B.; Demetrescu, I.; Mihai, G.V.; Enăchescu, M. The Design and Characterization of New Chitosan, Bioglass and ZnO-Based Coatings on Ti-Zr-Ta-Ag. *Coatings* **2023**, *13*, 493. [[CrossRef](#)]
47. Isola, G. Interface between Periodontal Tissues and Dental Materials: Dynamic Changes and Challenges. *Coatings* **2021**, *11*, 485. [[CrossRef](#)]
48. Kuralt, M.; Selmani Bukleta, M.; Kuhar, M.; Fidler, A. Bone and soft tissue changes associated with a removable partial denture. A novel method with a fusion of CBCT and optical 3D images. *Comput. Biol. Med.* **2019**, *108*, 78–84. [[CrossRef](#)]
49. Etman, M.K.; Bikey, D. Clinical performance of removable partial dentures: A retrospective clinical study. *Open J. Stomatol.* **2012**, *02*, 173–181. [[CrossRef](#)]
50. Greenstein, G.; Cavallaro, J.; Tarnow, D. Practical Application of Anatomy for the Dental Implant Surgeon. *J. Periodontol.* **2008**, *79*, 1833–1846. [[CrossRef](#)]
51. Yu, J.-M.; Kang, S.-Y.; Lee, J.-S.; Jeong, H.-S.; Lee, S.-Y. Mechanical Properties of Dental Alloys according to Manufacturing Process. *Materials* **2021**, *14*, 3367. [[CrossRef](#)]
52. Zhang, W.; Liaw, P.K.; Zhang, Y. Science and technology in high-entropy alloys. *Sci. China Mater.* **2018**, *61*, 2–22. [[CrossRef](#)]
53. Zhao, Y.; Zhao, P.; Li, W.; Kou, S.; Jiang, J.; Mao, X.; Yang, Z. The microalloying effect of ce on the mechanical properties of medium entropy bulk metallic glass composites. *Crystals* **2019**, *9*, 483. [[CrossRef](#)]
54. Perumal, G.; Grewal, H.S.; Pole, M.; Reddy, L.V.K.; Mukherjee, S.; Singh, H.; Manivasagam, G.; Arora, H.S. Enhanced Biocorrosion Resistance and Cellular Response of a Dual-Phase High Entropy Alloy through Reduced Elemental Heterogeneity. *ACS Appl. Bio Mater.* **2020**, *3*, 1233–1244. [[CrossRef](#)]
55. Castro, D.; Jaeger, P.; Baptista, A.C.; Oliveira, J.P. An Overview of High-Entropy Alloys as Biomaterials. *Metals* **2021**, *11*, 648. [[CrossRef](#)]
56. Cemin, F.; Luís Artico, L.; Piroli, V.; Andrés Yunes, J.; Alejandro Figueroa, C.; Alvarez, F. Superior in vitro biocompatibility in NbTaTiVZr(O) high-entropy metallic glass coatings for biomedical applications. *Appl. Surf. Sci.* **2022**, *596*, 153615. [[CrossRef](#)]
57. Ma, N.; Liu, S.; Liu, W.; Xie, L.; Wei, D.; Wang, L.; Li, L.; Zhao, B.; Wang, Y. Research Progress of Titanium-Based High Entropy Alloy: Methods, Properties, and Applications. *Front. Bioeng. Biotechnol.* **2020**, *8*, 603522. [[CrossRef](#)] [[PubMed](#)]
58. Edalati, P.; Floriano, R.; Tang, Y.; Mohammadi, A.; Pereira, K.D.; Luchessi, A.D.; Edalati, K. Ultrahigh hardness and biocompatibility of high-entropy alloy TiAlFeCoNi processed by high-pressure torsion. *Mater. Sci. Eng. C* **2020**, *112*, 110908. [[CrossRef](#)] [[PubMed](#)]
59. Geanta, V.; Voiculescu, I.; Vizureanu, P.; Victor Sandu, A. High Entropy Alloys for Medical Applications. In *Engineering Steels and High Entropy-Alloys*; IntechOpen: London, UK, 2020.
60. Drob, S.I.; Vasilescu, C.; Andrei, M.; Calderon Moreno, J.M.; Demetrescu, I.; Vasilescu, E. Microstructural, mechanical and anticorrosion characterisation of new CoCrNbMoZr alloy. *Mater. Corros.* **2016**, *67*, 739–747. [[CrossRef](#)]
61. Yang, W.; Liu, Y.; Pang, S.; Liaw, P.K.; Zhang, T. Bio-corrosion behavior and in vitro biocompatibility of equimolar TiZrHfNbTa high-entropy alloy. *Intermetallics* **2020**, *124*, 106845. [[CrossRef](#)]
62. Zhang, G.; Khanlari, K.; Huang, S.; Li, X.; Zhao, D.; Wu, H.; Cao, Y.; Liu, B.; Huang, Q. Dual-structured oxide coatings with enhanced wear and corrosion resistance prepared by plasma electrolytic oxidation on Ti-Nb-Ta-Zr-Hf high-entropy alloy. *Surf. Coat. Technol.* **2023**, *456*, 129254. [[CrossRef](#)]
63. Mazare, A.; Totea, G.; Burnei, C.; Schmuki, P.; Demetrescu, I.; Ionita, D. Corrosion, antibacterial activity and haemocompatibility of TiO₂ nanotubes as a function of their annealing temperature. *Corros. Sci.* **2016**, *103*, 215–222. [[CrossRef](#)]
64. Prodana, M.; Duta, M.; Ionita, D.; Bojin, D.; Stan, M.S.; Dinischiotu, A.; Demetrescu, I. A new complex ceramic coating with carbon nanotubes, hydroxyapatite and TiO₂ nanotubes on Ti surface for biomedical applications. *Ceram. Int.* **2015**, *41*, 6318–6325. [[CrossRef](#)]
65. Grigorescu, S.; Ungureanu, C.; Kirchgeorg, R.; Schmuki, P.; Demetrescu, I. Various sized nanotubes on TiZr for antibacterial surfaces. *Appl. Surf. Sci.* **2013**, *270*, 190–196. [[CrossRef](#)]

66. Berger, J.E.; Jorge, A.M.; Asato, G.H.; Roche, V. Formation of self-ordered oxide nanotubes layer on the equiatomic TiNbZrHfTa high entropy alloy and bioactivation procedure. *J. Alloys Compd.* **2021**, *865*, 158837. [[CrossRef](#)]
67. Yang, W.; Pang, S.; Liu, Y.; Wang, Q.; Liaw, P.K.; Zhang, T. Design and properties of novel Ti–Zr–Hf–Nb–Ta high-entropy alloys for biomedical applications. *Intermetallics* **2022**, *141*, 107421. [[CrossRef](#)]
68. Wang, S.; Wu, D.; She, H.; Wu, M.; Shu, D.; Dong, A.; Lai, H.; Sun, B. Design of high-ductile medium entropy alloys for dental implants. *Mater. Sci. Eng. C* **2020**, *113*, 110959. [[CrossRef](#)]
69. Iijima, Y.; Nagase, T.; Matsugaki, A.; Wang, P.; Ameyama, K.; Nakano, T. Design and development of Ti–Zr–Hf–Nb–Ta–Mo high-entropy alloys for metallic biomaterials. *Mater. Des.* **2021**, *202*, 109548. [[CrossRef](#)]
70. Nagase, T.; Iijima, Y.; Matsugaki, A.; Ameyama, K.; Nakano, T. Design and fabrication of Ti–Zr–Hf–Cr–Mo and Ti–Zr–Hf–Co–Cr–Mo high-entropy alloys as metallic biomaterials. *Mater. Sci. Eng. C* **2020**, *107*, 110322. [[CrossRef](#)]
71. Hashimoto, N.; Al-Zain, Y.; Yamamoto, A.; Koyano, T.; Kim, H.Y.; Miyazaki, S. Novel beta-type high entropy shape memory alloys with low magnetic susceptibility and high biocompatibility. *Mater. Lett.* **2021**, *287*, 129286. [[CrossRef](#)]
72. Wang, W.; Yang, K.; Wang, Q.; Dai, P.; Fang, H.; Wu, F.; Guo, Q.; Liaw, P.K.; Hua, N. Novel Ti–Zr–Hf–Nb–Fe refractory high-entropy alloys for potential biomedical applications. *J. Alloys Compd.* **2022**, *906*, 164383. [[CrossRef](#)]
73. Gurel, S.; Yagci, M.B.; Bal, B.; Canadinc, D. Corrosion behavior of novel Titanium-based high entropy alloys designed for medical implants. *Mater. Chem. Phys.* **2020**, *254*, 123377. [[CrossRef](#)]
74. Tünten, N.; Canadinc, D.; Motallebzadeh, A.; Bal, B. Microstructure and tribological properties of TiTaHfNbZr high entropy alloy coatings deposited on Ti–6Al–4V substrates. *Intermetallics* **2019**, *105*, 99–106. [[CrossRef](#)]
75. Hori, T.; Nagase, T.; Todai, M.; Matsugaki, A.; Nakano, T. Development of non-equiatomic Ti–Nb–Ta–Zr–Mo high-entropy alloys for metallic biomaterials. *Scr. Mater.* **2019**, *172*, 83–87. [[CrossRef](#)]
76. Shittu, J.; Pole, M.; Cockerill, I.; Sadeghilaridjani, M.; Reddy, L.V.K.; Manivasagam, G.; Singh, H.; Grewal, H.S.; Arora, H.S.; Mukherjee, S. Biocompatible High Entropy Alloys with Excellent Degradation Resistance in a Simulated Physiological Environment. *ACS Appl. Bio Mater.* **2020**, *3*, 8890–8900. [[CrossRef](#)] [[PubMed](#)]
77. Yu, B.; Juma, T.; Wang, H.; Bao, X.; Cao, X.; Wang, Z.; Wang, R.; Yang, X.; Ning, T.; Liang, G.; et al. Development of new Ti₅₀Zr₂₅Nb₂₀Cu₅–Ag high-entropy alloys with excellent antibacterial property, osteo-conductivity and biocompatibility in vitro and in vivo. *J. Mater. Sci. Technol.* **2023**, *141*, 209–220. [[CrossRef](#)]
78. Todai, M.; Nagase, T.; Hori, T.; Matsugaki, A.; Sekita, A.; Nakano, T. Novel TiNbTaZrMo high-entropy alloys for metallic biomaterials. *Scr. Mater.* **2017**, *129*, 65–68. [[CrossRef](#)]
79. Riivari, S.; Närvä, E.; Kangasniemi, I.; Willberg, J.; Närhi, T. Focal adhesion formation of primary human gingival fibroblast on hydrothermally and in-sol-made TiO₂-coated titanium. *Clin. Implant. Dent. Relat. Res.* **2023**, *25*, 583–591. [[CrossRef](#)] [[PubMed](#)]
80. Yang, Y.; Wang, X.; Wang, Y.; Hu, X.; Kawazoe, N.; Yang, Y.; Chen, G. Influence of Cell Spreading Area on the Osteogenic Commitment and Phenotype Maintenance of Mesenchymal Stem Cells. *Sci. Rep.* **2019**, *9*, 6891. [[CrossRef](#)]
81. Akmal, M.; Hussain, A.; Afzal, M.; Lee, Y.I.; Ryu, H.J. Systematic study of (MoTa) NbTiZr medium- and high-entropy alloys for biomedical implants—In vivo biocompatibility examination. *J. Mater. Sci. Technol.* **2021**, *78*, 183–191. [[CrossRef](#)]

Disclaimer/Publisher’s Note: The statements, opinions and data contained in all publications are solely those of the individual author(s) and contributor(s) and not of MDPI and/or the editor(s). MDPI and/or the editor(s) disclaim responsibility for any injury to people or property resulting from any ideas, methods, instructions or products referred to in the content.